

Article

Predicting the Effect of Hull Roughness on Ship Resistance Using a Fully Turbulent Flow Channel

Roberto Ravenna ^{1,*}, Ryan Ingham ², Soonseok Song ³, Clifton Johnston ², Tahsin Tezdogan ¹, Mehmet Atlar ¹ and Yigit Kemal Demirel ⁴

¹ Department of Naval Architecture, Ocean and Marine Engineering, University of Strathclyde, Glasgow G1 0LZ, UK

² Department of Mechanical Engineering, Faculty of Engineering, Dalhousie University, Halifax, NS B3H 4R2, Canada

³ Department of Naval Architecture & Ocean Engineering, College of Engineering, Inha University, Incheon 22212, Republic of Korea

⁴ 160 Bothwell Street, Glasgow G2 7EA, UK

* Correspondence: roberto.ravenna@strath.ac.uk

Abstract: The consequences of poor hull surface conditions on fuel consumption and emissions are well-known. However, their rationales are yet to be thoroughly understood. The present study investigates the hydrodynamics of fouling control coatings and mimicked biofouling. Novel experimental roughness function data were developed from the “young” fully turbulent flow channel facility of the University of Strathclyde. Different surfaces, including a novel hard foul-release coating, were tested. Finally, the performance of a benchmark full-scale containership was predicted using Granville’s similarity law scaling calculations. Interestingly, the numerical predictions showed that the novel hard foul-release coating tested had better hydrodynamic performance than the smooth case. A maximum 3.79% decrease in the effective power requirements was observed. Eventually, the results confirmed the practicality of flow channel experiments in combination with numerical-based methods to investigate hull roughness effects on ship resistance and powering. The present study can also serve as a valuable guide for future experimental campaigns using the fully turbulent flow channel facility of the University of Strathclyde.

Keywords: fully turbulent flow channel (FTFC); roughness effect; fouling control coatings (FCCs); KRISO containership (KCS); Granville’s similarity law; ship resistance and powering



Citation: Ravenna, R.; Ingham, R.; Song, S.; Johnston, C.; Tezdogan, T.; Atlar, M.; Demirel, Y.K. Predicting the Effect of Hull Roughness on Ship Resistance Using a Fully Turbulent Flow Channel. *J. Mar. Sci. Eng.* **2022**, *10*, 1863. <https://doi.org/10.3390/jmse10121863>

Academic Editor: Kamal Djidjeli

Received: 1 November 2022

Accepted: 24 November 2022

Published: 2 December 2022

Publisher’s Note: MDPI stays neutral with regard to jurisdictional claims in published maps and institutional affiliations.



Copyright: © 2022 by the authors. Licensee MDPI, Basel, Switzerland. This article is an open access article distributed under the terms and conditions of the Creative Commons Attribution (CC BY) license (<https://creativecommons.org/licenses/by/4.0/>).

1. Introduction

A ship’s hull surface condition is crucial to its hydrodynamic performance [1]. Hence, choosing the right fouling control coating (FCC) and drydock strategies for a vessel can offer significant economic and environmental advantages. Furthermore, improving hull performances associated with surface conditions enables the vessels to comply with IMO regulations [2], such as the operating expense index (OPEX), Energy Efficiency Existing Ship Index (EEXI) and the novel Carbon Intensity Indicator (CII). Although extensive literature was dedicated to assessing the effect of hull roughness on ship resistance, as summarised by [3], the understanding of the hydrodynamics behind the problem is still limited.

Granville method [4,5] can accurately predict the hull roughness effect on ship resistance, provided that the roughness function is known. Such method is based on the turbulent boundary layer similarity law scaling technique. The roughness function is the difference between the velocities in the boundary layer between a rough surface and a hydraulically smooth reference surface [6]. Furthermore, Granville’s method owes its merit to its robustness and practicality [7]. Additionally, it allows to predict the roughness effect on the frictional resistance for ships of arbitrary lengths and speeds [8].

The specific roughness function models can effectively represent hull surface conditions. However, no universal roughness function can represent all surfaces. Therefore, the roughness function can be seen as the hydrodynamic fingerprint of any given surface. Consequently, several theoretical and experimental methods have been developed for determining the roughness function of rough surfaces. Ref. [9] gave a comprehensive overview of these experimental methods and their advantages and disadvantages, and [10] presented a historical overview of the experimental facilities used in hull coating hydrodynamic tests. Among the literature, a recurrent successful alternative to determine the roughness functions of given surfaces is a fully turbulent flow channel (FTFC) facility. By offering rapid experimental turn-around times combined with high Reynolds numbers, FTFCs can provide reliable results combined with significant financial savings.

Therefore, several investigators have studied turbulent channel flow experimentally. For example, Dean et al. [11] provided us with a widely adopted reference equation. However, much of this research had focused on the Reynolds-number dependence of the skin friction and the mean flow, as reported in [12]. In [13], an investigation was conducted on the skin-friction behaviour in the transitionally rough regime using a turbulent channel flow facility installed in the United States Naval Academy using Granville's indirect method for pipes [14]. Results were analogous to the Nikuradse-type roughness function [15], which were obtained when investigating the effect of wall roughness on turbulent flows by measuring the pressure drop across a pipe. Additionally, in a recent investigation on the effect of hull roughness on ship resistance using a FTFC, ref. [16] recommended a procedure to estimate the effect of roughness on ship hull resistance based on Granville's procedure [14] by using the experimentally determined database for roughness functions of rough surfaces. Recently, ref. [17] conducted skin friction measurements with an FTFC on two different sizes of silicon carbide particles (i.e., F220 silicon carbide particles with an average grain size of 53–75 μm and F80 silicon carbide particles with an average grain size of 150–212 μm), proving that roughness amplitude parameters alone are not enough to explain the hydrodynamic performance of surfaces. Furthermore, ref. [18] developed roughness functions for different antifouling coatings by conducting flow cell experiments and predicted the frictional performance of a KVLCC2 hull (Korean Very Large Crude Carrier) model case.

Within the framework of the above literature review, it is clear that the most rational current approach to tackling the effect of ship hull roughness, including biofouling, is to combine experimental and numerical methods. This would require determining the roughness functions using experimental methods, such as cost-effective and practical FTFCs. Therefore, this study aims to obtain new roughness functions for a novel hard foul-release coating, other commonly used marine coatings, and mimicked biofouled hull conditions. Furthermore, the purpose of this paper was to demonstrate the advantages of FTFC experiments to predict the effect hull roughness on full-scale ship resistance and powering. In fact, an important objective was to use the FTFC of the UoS, which is a more practical facility than, e.g., a towing tank. To the best of author's knowledge, only limited (and unpublished) research has been conducted using the FTFC of the UoS. Hence, the sophisticated new FTFC designed and custom-built [19] at the University of Strathclyde (UoS) was used in the present study. While the facility supports drag reduction studies, another aim of such a facility is to contribute to the international database of the roughness functions for different FCCs and biofouling, as recommended, e.g., by the 21st ITTC Surface Treatment Committee [20]. Therefore, different FCCs produced by Graphite Innovation and Technologies [21], including antifouling, foul-release and barrier resin coatings and the newly developed hard foul-release coating (FR02) were tested in the FTFC. Roughness functions were developed from FTFC tests for widely adopted sandpaper-like surfaces mimicking biofouled conditions (medium light slime and medium slime) as similarly done in towing tests [22]. Furthermore, the roughness function developed for a sandpaper-like surface (*Sand 220*) from the FTFC experiments was compared with previous towing tank

tests. Finally, the present study also aims to confirm the robustness of Granville’s method to predict the effect of hull roughness on ship resistance and powering.

The remaining of the paper is structured as follows: Section 2 presents the methodology adopted, including the experimental setup, roughness functions development, Granville’s similarity law scaling procedure, and experimental uncertainty analysis. Section 3 of the paper discusses the current experimental and numerical investigation results. The novel roughness functions of the test surfaces are presented and used to predict the variation of resistance coefficients and effective power for the full-scale KRISO Container Ship (KCS) hull. Section 4 presents the conclusions, final remarks, and recommendations for future studies.

2. Methodology

2.1. Approach

Figure 1 shows a schematic illustration of the experimental and numerical methodology adopted to investigate the roughness effects of marine coatings and mimicked biofouling on the well-known KRISO Container Ship (KCS) [23].

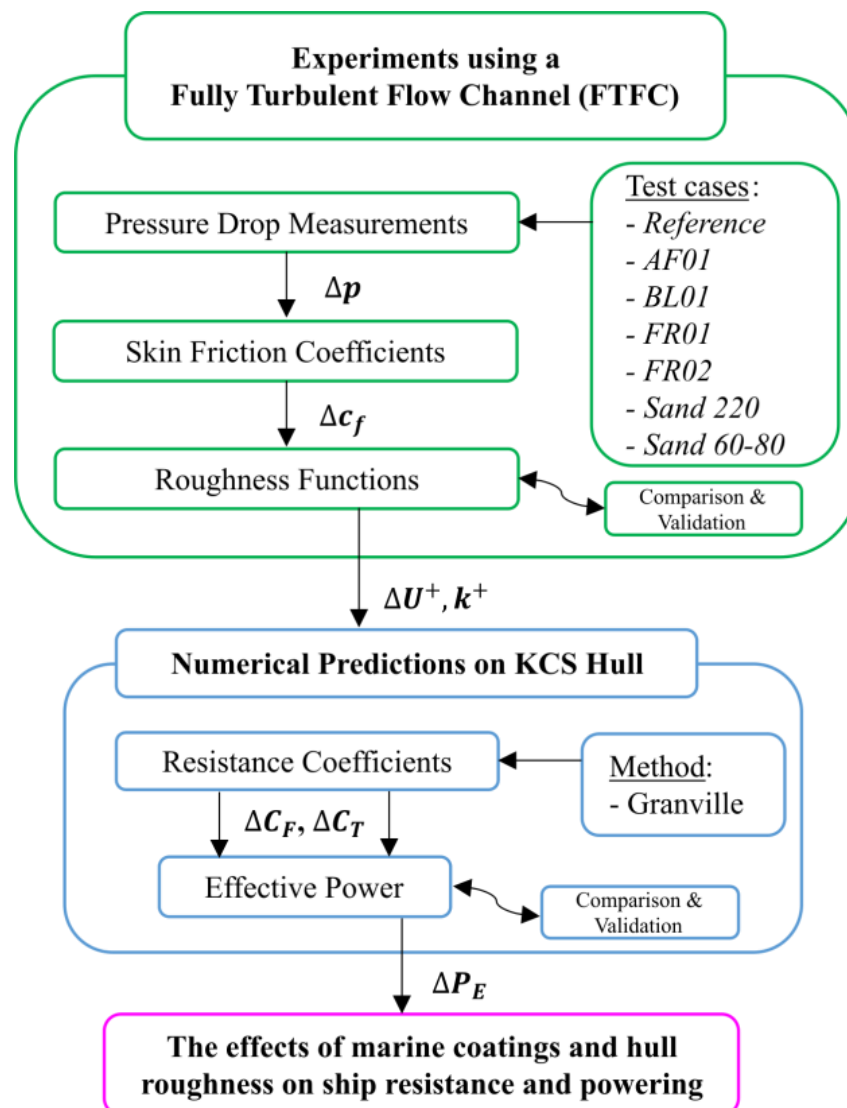


Figure 1. Schematic illustration of the methodology adopted.

Drag characterisation of arbitrary rough surfaces on flat plates can be evaluated by the indirect method for pipes [14] that uses the pressure drop Δp , which can be measured along the coatings (i.e., the pressure drop method). The FTFC was used to determine the skin friction coefficients c_f , by measuring the pressure drop Δp on the test surfaces. Eventually, the roughness functions obtained for the test surfaces (i.e., roughness functions, ΔU^+ , roughness Reynolds numbers k^+ , roughness length scale, k , etc.), were compared and validated [24], and then embedded in numerical methods to predict the effect of such surfaces on ship resistance and powering.

Consequently, the boundary layer similarity law scaling procedure of Granville [4,5] was adopted in the present study to predict the effect of the test surfaces on the full-scale KCS hull. Additionally, the resistance coefficient results of the numerical predictions were compared and validated across similar studies assessing the KCS resistance in smooth and rough conditions [25,26]. Finally, the variations in effective power, ΔP_E due to each test surface were estimated to give an immediate understanding of the effects of marine coatings and hull roughness on ship resistance and powering. Comparison and validation of the ΔP_E values obtained were conducted among similar studies [27].

2.2. Experimental Setup

2.2.1. Fully Turbulent Flow Channel

The University of Strathclyde’s Fully Turbulent Flow Channel (FTFC), as shown in Figure 2a, was designed and installed at the KHL of the NAOME Dept (UoS) to conduct a series of measurements for various types of fouling control coatings and rough surfaces in the freshly applied condition. Delivered to the UoS in 2019, the FTFC is a closed-circuit flow channel that can accommodate two opposing panels in its test section (Figure 2b) located downstream of a single centrifugal pump. The channel has a speed range of 1.5–13.5 m/s, thus able to reach high Reynolds numbers $Re_M \approx 3.0 \cdot 10^5$. Re_M is the channel height-based Reynolds number based on mean bulk velocity of the flow, U_M . The resulting wall shear stress over 300 Pa in the facility with smooth panels. This creates wall shear stress conditions that are similar to average conditions on a smooth ship, 150 m in length, travelling at up to 17 m s^{-1} (33 knots), as observed by [28].

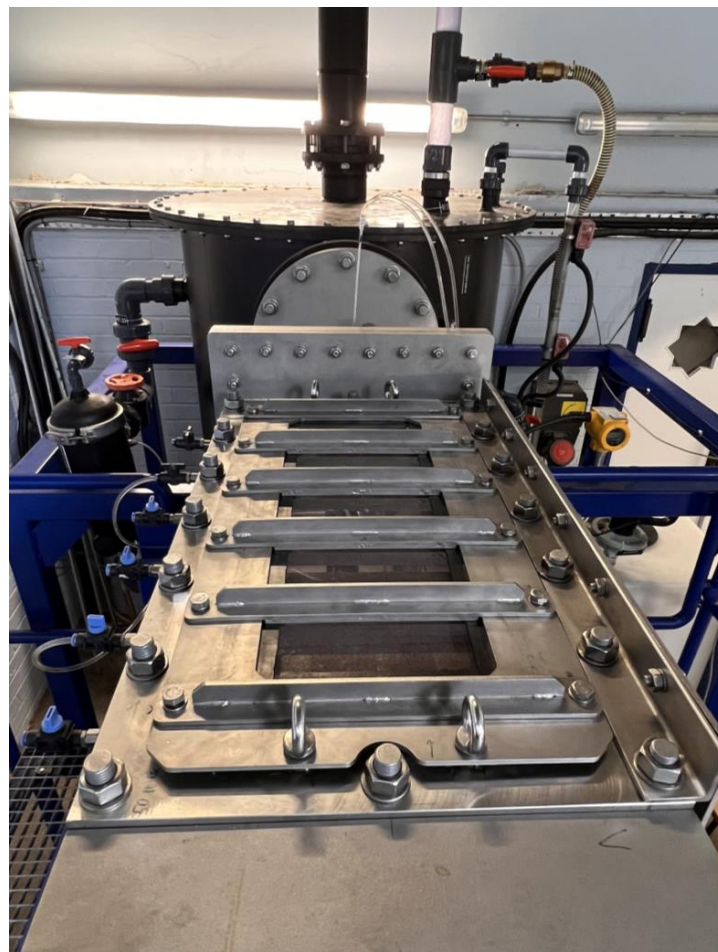
The UoS FTFC ensures the development of a two-dimensional flow at its test section located at the downstream (tail end) of the upper limb, where the flow becomes fully turbulent. This is due to its features, e.g., a relatively large test section with a channel height (22.5 mm), an aspect ratio of 8:1, water speed (13.5 m/s) and a laser-based measurement access as well as a capability for circulating seawater, Table 1 summarises the main particulars of the FTFC upper limb section. The volume of the system (main tank, auxiliary tank, etc.) is 2.58 m^3 . For information on the FTFC design, operation and calibration, the reader is advised to see [19].

Table 1. Main particulars of the FTFC upper limb.

Name	Symbol	Unit	Value
Length (Tolerance)	l	mm	3000 (± 0.05)
Height (Tolerance)	h	mm	22.5 (± 0.05)
Beam (Tolerance)	b	mm	180 (± 0.05)
Speed range	U	m/s	1.5–13.5
Flow rate	Q	l/s	10–60
Channel height-based Reynolds number	Re_M	-	$\approx 3.0 \cdot 10^5$
Material	-	-	Stainless steel (316 L)
Centrifugal Pump power	P	kW	22



(a)



(b)

Figure 2. The Fully Turbulent Flow Channel (FTFC) of the University of Strathclyde (UoS). (a) On-site picture of the FTFC. (b) Top view of the test section accommodating a couple of transparent panels.

2.2.2. Test Panels Design and Preparation

In the present experimental campaign, four different types of FCCs were tested in the FTFC, including the newly developed hard foul-release coating (FR02) manufactured by GIT [21] and marine coatings type that are commonly used in the shipping industry manufactured at Dalhousie University (DU), i.e., a self-polishing antifouling coating (AF01), a gelcoat barrier coating (BL01), and a soft foul-release coating (FR01). Furthermore, two sandpaper-like surfaces mimicking slime biofouling, i.e., *Sand 220* (medium light slime) and the coarser, *Sand 60-80* (medium slime) manufactured at the UoS, were tested. The coated panels (Figure 3a) were tested along with an uncoated “control surface” or the “reference” to represent hydraulically smooth surfaces, Figure 3b. Additionally, the sanded control panels (*Sand 220* and *Sand 60-80*) and the reference panel were of acrylic (i.e., Polymethyl Methacrylate, PMMA) sheets. On the other hand, high-density polyethylene was used as the material to manufacture the test panels for marine coating applications.



Figure 3. Surfaces tested in the FTFC. (a) Test panels coated with different fouling control coatings and sand grit. (b) Uncoated smooth reference panel.

Table 2 describes the dimensions of the test panels, while a breakdown of the type of each marine coating applied and the method of application is provided in Table 3. It is of note that in Table 3, the arithmetic mean roughness, R_a , for the FCCs was measured using the Surtronic 25 gauge by Taylor & Hobson over a cut-off length of 0.8 mm, while the R_a for the sanded rough surfaces was measured using the TQC roughness measurement gauge. The filtering is often carried out because the long wavelength component of the roughness is not expected to contribute significantly to the frictional drag. However, it is worth noting that the selection of the optimum cut-off length in order to characterise a surface in a hydrodynamic sense is still unresolved [28]. A review article by [29] discusses this issue in the context of ship hull paints. E.g., the Gaussian filter with a 2.5 mm cut-off length is used by [30] whilst [28] use a 5 mm cut-off length for similar hull paints. Further surface statistics studies could be carried in future studies. Different cut-off lengths could be used to filter the measured data. The surfaces were profiled with an OSP100

optical profilometer (Uniscan Instruments Ltd., Buxton, UK) utilising laser interferometry. The optical laser sensor was adjusted on the two-axis traverse with positioning range of 90 mm × 40 mm. Eighty linear profiles were measured at a scanning speed of 15 mm/s giving a total of 3600 points on the x axis. Representative images of the surface topography for the test surfaces are presented in Appendix A.

Table 2. Dimensions of the FTFC test panels.

Dimension	[mm]
Inner length	599
Inner breadth	218
Inner thickness	14
Outer length	662
Outer breadth	282
Outer thickness	16
Tolerance	0.1

Table 3. Overview of each test panel set. Similar test surfaces can be found in [31].

Panel Set Name	Description (Prepared/ Manufactured by)	Panel Material	Coating Type (Topcoat, Underlayers)	Method of Application (Topcoat, Underlayers)	Colour	Arithmetic Mean Roughness (R _a) [µm]
Reference	Smooth reference panel (UoS)	Acrylic	N/A	N/A	Transparent	0.04
AF01	Self-Polishing antifouling coating (DU)	High Density Polyethylene	Self-polishing antifouling, anticorrosive primer	Airless spray, Airless spray	Red matt	0.96
BL01	Gelcoat barrier coating (DU)	High Density Polyethylene	Vinyl ester resin barrier	Airless spray	Green matt	1.44
FR01	Soft foul-release coating (DU)	High Density Polyethylene	Fluoropolymer/ silicone foul-release, elastomeric tie coat, anticorrosive primer	Roller, Roller, Airless spray	Blue lucid	0.10
FR02	Hard foul-release coating (DU/GIT)	High Density Polyethylene	Hard foul-release, anticorrosive primer	Airless spray, Airless spray	White lucid	0.22
Sand 220	Medium light slime surface (UoS)	Acrylic	Sanded rough, Aluminium oxide sand grit 220	Scattering, Roller resin	Gray matt	294
Sand 60-80	Medium slime surface (UoS)	Acrylic	Sanded rough, Aluminium oxide sand grit 60-80	Scattering, Roller resin	Brown matt	509

2.2.3. Pressure Drop Measurements

The UoS’ FTFC facility is fitted with six pressure taps on the side opposite the laser window to measure the pressure drop (Figure 4).

Pressure taps 2–5 were chosen for pressure drop measurements to avoid pressure waves and noise disturbances at the ends of the measuring section. In fact, taps 2–5 also provided the lowest uncertainty in pressure drop values at the mid-range pump frequency (16 Hz) [19]. Each pair of taps can be connected to a differential pressure transducer with a range of 0–400 mbar via plastic hoses. It is of note that the pressure taps are 120 mm apart from each other, and the pressure drop Δ*p* is used in relation to the streamwise linear distance Δ*x* to assess the skin friction of the surfaces, according to the following formulae from Equations (1)–(4) [11]:

$$\text{Skin friction coefficient : } c_f = \frac{\tau_w}{\frac{1}{2}\rho U_M^2} \tag{1}$$

$$\text{Wall shear stress : } \tau_w = -\frac{D_h \Delta p}{4 \Delta x} \tag{2}$$

$$\text{Hydraulic diameter : } D_h = \frac{2hb}{h+b} \tag{3}$$

$$\text{Reynolds number : } Re_M = \frac{U_M h}{\nu} \tag{4}$$

where h and b are, respectively, the channel height ($h = 22.5$ mm) and channel width ($b = 180$ mm), ρ , the water density, and U_M , the mean bulk velocity of the flow in the test section. The water density, ρ , is specified based on the formulae provided by [31], including the correction for the temperature of the channel flow, which is continuously recorded by the channel sensor. Furthermore, the pressure drop measurements were conducted for a range of mean bulk velocities, U_M , calculated by using the data obtained from the magnetic flowmeter. For each set of test panels, the full range of pump frequencies was assessed (5–40 Hz) to give 36 different mean bulk velocity values (approx. 1.5–13.5 m/s). The variation of the mean bulk velocity at the test section of the FTFC with the smooth reference (uncoated) panel against the pump frequency (rotation per second) is shown in Figure 5. Future studies could consider the kinetic Reynolds number (i.e., Valensi number) to correlate the oscillating frequency with the flow velocity.



Figure 4. Pressure taps distribution numbered from 1 to 6 (left to right) on the test section of the FTFC.

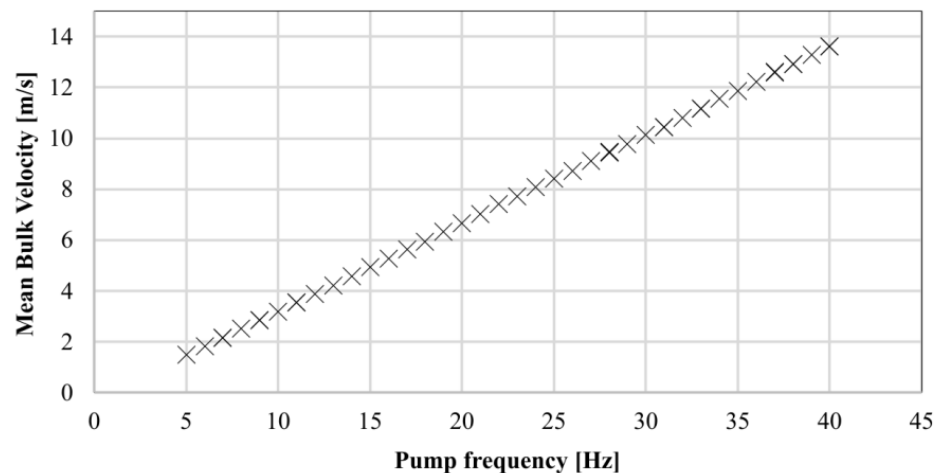


Figure 5. Centrifugal pump frequencies and corresponding mean bulk velocities at the test section of the FTFC with the hydraulically smooth reference (uncoated) panel.

2.3. Roughness Functions Determination

Different surfaces are characterised by different roughness functions to be modelled experimentally [5]. For Roughness Function (or velocity loss function), ΔU^+ , is intended further retardation of flow in the boundary layer over a rough surface due to the physical roughness of that surface, which manifests itself as additional drag relative to a smooth surface. Therefore, the roughness effect can also be seen as a downward shift of the non-dimensional velocity profile in the turbulent boundary layer log-law region (i.e., variance in the local velocities). The non-dimensional velocity profile (U^+) in the log-law region for a rough surface can be written by (5) [32]:

$$U^+ = \frac{1}{\kappa} \ln y^+ + B - \Delta U^+ \tag{5}$$

where, κ is the von-Karman constant, y^+ is the non-dimensional normal distance from the boundary ($y^+ = yU_\tau/\nu$), B is the smooth wall log-law intercept.

The roughness function, ΔU^+ is a function of the roughness Reynolds number, k^+ , which is defined by Equation (6) [33]:

$$k^+ = \frac{kU_\tau}{\nu} \tag{6}$$

where, k is the roughness lengths scale of the surface, and U_τ is the friction velocity based on wall shear stress defined by Equation (7) [34]:

$$U_\tau = \sqrt{\tau_w/\rho} \tag{7}$$

where, τ_w is the wall shear stress.

For this study, the indirect method for characterizing the drag of an arbitrarily rough surface on a fully developed pipe flow proposed by [14] is used to calculate the roughness function ΔU^+ and roughness Reynolds number k^+ for each coating as follows:

$$\text{Roughness function : } \Delta U^+ = \sqrt{\frac{2}{c_{f,s}}} - \sqrt{\frac{2}{c_{f,r}}} \tag{8}$$

$$\text{Roughness Reynolds number : } k^+ = \frac{1}{\sqrt{2}} Re_{M,r} \sqrt{c_{f,r}} \frac{k}{D_h} \tag{9}$$

where, $c_{f,s}$ and $c_{f,r}$ are the skin friction factors measured in the smooth and rough pipes, respectively, at the same value of $Re_M \sqrt{c_f}$, and k is the roughness length scale. It is of note that the roughness length scale values, k , were selected so that the roughness function models obtained were in agreement with the Nikuradse [15,33] or Colebrook type [35]. Furthermore, the hydraulic diameter, D_h of the channel was calculated by Equation (3) as in [14]. Finally, Granville’s method was adopted to predict the effect of the test surfaces on the KCS full-scale hull. Notably, the process for Granville’s scale-up method [4,5] is explained in detail in [6]. An in-house code was developed to conduct Granville’s scaling procedure based on the roughness function data obtained in this study.

2.4. Experimental Uncertainty Analysis

The uncertainties of the measurements in the FTFC tests, Table 4, were assessed following the ITTC-recommended procedures [36]. The standard errors for the coefficient of friction were calculated based on four to six replicate runs of the *FR01* panel at the minimum and maximum flow velocities, respectively. The precision uncertainty in the skin friction coefficient was calculated at a 95% confidence interval by multiplying the standard error by the two-tailed t values ($t = 3.182, 2.571$) for three to five degrees of freedom, according to [37]. The accuracy of the differential pressure sensor is $\pm 0.075\%$ and the accuracy of the magnetic flow meter was $\pm 0.2\%$ according to the manufacturer’s

specifications, Table 5. The total uncertainty was calculated using Equation (10) and typical error propagation techniques [38]:

$$(U_A)^2 = (B_A)^2 + (P_A)^2 \tag{10}$$

where B_A is the bias uncertainty limit, P_A is the precision uncertainty limit and U_A is the total uncertainty. The overall uncertainty in the roughness function, ΔU^+ is $\pm 14.4\%$ or 0.04 (whichever is larger) at the lowest Re_M , $\pm 6.5\%$ or 0.04 (whichever is larger) at the highest Re_M . The total bias limit and precision limit for the skin friction coefficients c_f were combined using Equation (10) to give a total uncertainty of $\pm 0.74\%$ at the lowest Re_M and $\pm 0.52\%$ at the highest Re_M , Figure 6. For comparison, the high Reynolds number turbulent flow facility at the US Naval Academy achieved a relatively similar level of uncertainty, with their skin friction data being $\pm 1.2\%$ at Re_M between $4.0 \cdot 10^4 - 3.0 \cdot 10^5$ [28].

Table 4. Uncertainty in the c_f with 95% confidence level at the highest speed.

		P_A	B_A	U_A
c_f	Absolute	$1.23 \cdot 10^{-5}$	$1.44 \cdot 10^{-5}$	$1.89 \cdot 10^{-5}$
	Relative	$\pm 0.34\%$	$\pm 0.4\%$	$\pm 0.52\%$

Table 5. Manufacturer specification of all measuring instruments.

Measuring and Control Instrument	Accuracy
Magnetic flow meter	$\pm 0.2\%$
Differential pressure sensor	$\pm 0.075\%$
Pressure sensor	$\pm 0.5\%$
Temperature transmitter with resistance thermometer	$\pm 0.1\%$

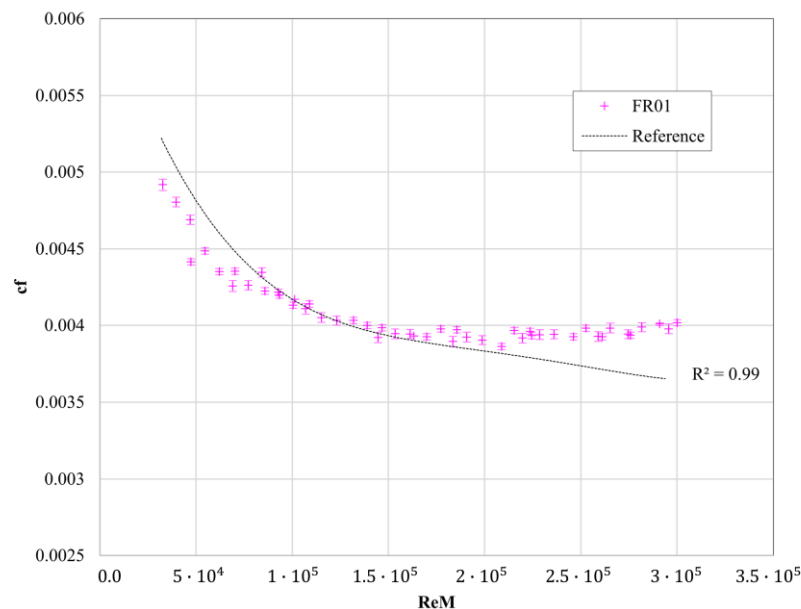


Figure 6. Skin-friction coefficient, c_f , vs. Reynolds number, Re_M for the FR01 soft foul-release coating. The error bars represent the overall uncertainty at 95% confidence level.

3. Results and Discussion

3.1. Fully Turbulent Flow Channel Experiments

3.1.1. Wall Shear Stress, τ_w

The wall shear stress of each panel set was calculated by Equation (2) based on the hydraulic diameter of the channel defined in Equation (3) and the resulting longitudinal

pressure drop ($\Delta p/\Delta x$). In Figure 7 a plot of τ_w vs. flow speed for each panel set is shown, including the 1957 ITTC skin friction formulation for a 232.5 m long flat plate. As shown, the wall shear stress of a 232.5 m long flat plate representing the full-scale KCS at ship speed of 24 knots (12.35 m/s) can be achieved in the FTFC at a considerably low flow speed (4.8–7.2 m/s). In fact, the horizontal dashed red line represents the constant τ_w achieved by KCS at 24 knots. This line crosses the τ_w curves of the FTFC tested panels at considerably lower velocities than the ITTC curve. In other words, at a constant speed of 24 knots (indicated by the vertical dashed red line at 12.35 m/s), the τ_w values of the tested panels in the FTFC are much higher than the value from the ITTC formulation. Therefore, the results from the FTFC can be accurately analogised to the turbulent boundary layer formed on a ship’s hull at cruising speed. In fact, the FTFC enables the measurement of much higher flow speeds and τ_w values that would not be otherwise achievable in a typical towing tank with flat friction test plates.

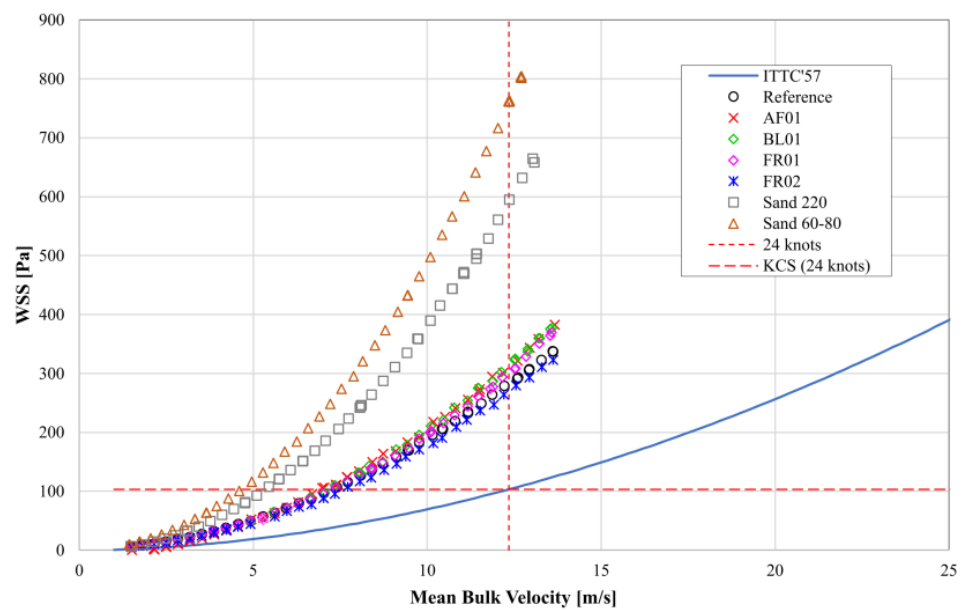


Figure 7. Wall shear stress achieved in FTFC compared to a 232.5 m long flat plate using the ITTC formulation.

Overall, the wall shear stress trend of all the FCCs surfaces tested is quite similar. The very subtle differences are related to minor differences in surface roughness that likely arise from application rather than being inherent in any differences in the coatings themselves. Similar observations were made in [28].

3.1.2. Skin Friction Coefficients, c_f

Figure 8 shows the skin friction coefficient, c_f of each test surface plotted against the Reynolds number, Re_M compared to the hydraulically smooth acrylic panel and reference data taken from [39]. It is of note that the almost unitary R^2 value in Figure 8 refers to the polynomial trendline fitted for the experimental reference data. Interestingly, all the test surfaces had skin friction coefficient values beneath the smooth friction line at low Reynolds numbers except for the sanded surfaces. It can be noted that the AF01 displayed unique frictional coefficients behaviour below values of $Re_M < 10^5$, which its surface condition appearance could not explain. The FR01 and BL01 coatings had skin friction curves that followed the behaviour of the smooth acrylic reference panel up until $Re_M = 2 \cdot 10^5$ where the surfaces showed an increase in skin friction compared to the reference surface. Furthermore, all the surfaces had skin friction coefficient values above the smooth friction line at higher Re values ($Re_M > 2 \cdot 10^5$) except for the AF01 and FR02 surfaces. In fact, AF01 and FR02 were the only surfaces to maintain a lower skin friction coefficient than the

smooth reference surface over the entire Reynolds number range ($3 \cdot 10^4 < Re_M < 3 \cdot 10^5$). These coatings (AF01 and FR02) probably have lower friction than the smooth reference because their surface is amphiphilic and hydrophobic, while the reference is neutral. It is of note that each panel set separated from the hydraulically smooth condition at slightly different values of Reynolds numbers. On the other hand, Sand 220 and Sand 60-80 had a neat increase in skin friction from the smooth reference panel. As expected, the increase in skin friction is greater for the coarsest of the two surfaces, Sand 60-80, than the smoothest, Sand 220. It is of note that each panel set separated from the hydraulically smooth condition at slightly different values of Reynolds numbers. On the other hand, Sand 220 and Sand 60-80 had a neat increase in skin friction from the smooth reference panel. As expected, the increase in skin friction is greater for the coarsest of the two surfaces, Sand 60-80, than the smoothest, Sand 220.

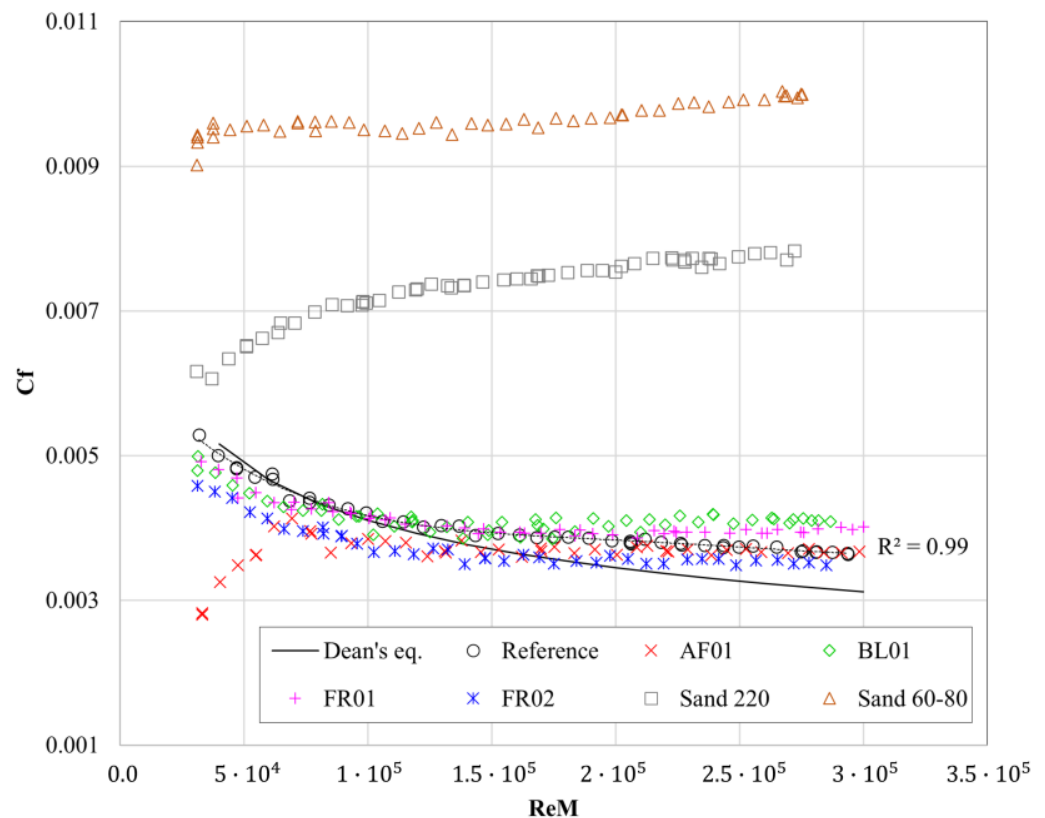


Figure 8. Skin friction coefficients (c_f) vs. Reynolds number (Re_M) for all marine coating surfaces.

As discussed, the AF01 and FR02 coatings had an interesting decrease in skin friction from the smooth reference panel. The authors believe that (regardless of experimental errors) this virtuous behaviour may illustrate the impact of the application method as well as each coating's ability to behave like a smoother surface under high flow conditions than the smooth reference surface. In fact, the chemistry of the surface and the application method affect the surface roughness and hence the frictional resistance. In other words, as discussed in the methodology section, it is also important to note that these surfaces were applied in a largely isolated (i.e., laboratory) environment which is not representative of the conditions of a real-world coating application in a dockyard. In fact, a dockyard environment can be subject to a variety of external factors, including high winds, temperature, and pre-existing hull roughness (macro roughness). Therefore, the coating surfaces presented in this study and those compared in other studies, especially the coatings that were airless sprayed (FR02 & AF01) should therefore be taken as a better finish than one that would be achieved on the surface of a ship in drydock [28,40].

It is worth noting that all the FCCs tested exhibited decreasing c_f with increasing Reynolds number until $Re_M < 10^4$. This is indicative of surfaces that have not yet reached the fully rough flow regime. For $Re_M > 10^4$ the c_f s of the FCCs become independent of Reynolds number. This could be a proof of the Reynolds number of these tests being high enough to achieve fully rough behaviour. On the other hand, for the *Sand 220* and *Sand 60-80* that were tested at the same Reynolds numbers, this was not the case. In fact, it could be indicative of a fundamental change in flow regimes. *Sand 220* and *Sand 60-80* do not display typical fully rough behaviour at least over the range of Reynolds number assessed here. Instead, c_f continues to increase with Reynolds number over the entire Reynolds number range.

3.1.3. Roughness Function Models

As discussed in the methodology section (Section 2), provided that the roughness functions of the test surfaces are known, Granville's similarity law can be used to predict the effect of hull roughness on ship resistance. Once the roughness functions have been calculated, they were directly compared with both Colebrook-type [41] and Nikuradse-type [15] roughness functions. Furthermore, the roughness functions of the sandpaper-like surfaces were compared for validation purposes with results obtained from other studies [24]. In fact, previous flat plate towing tank experiments conducted for the same surface roughness (*Sand 220*) were used for comparison to the present results, Figure 9. These towing tank experiments, Figure 10, were conducted on a stainless steel flat plate (dimensions 1.495×0.588 m) at a range of speed (1.5–4.5 m/s) as used in [24,42]. The towing tank facilities of Kelvin Hydrodynamics Laboratory (KHL) of the University of Strathclyde were used. In that occasion, the same $k = 1.532 \cdot 10^{-4}$ m was used to collapse the roughness function on the Nikuradse reference.

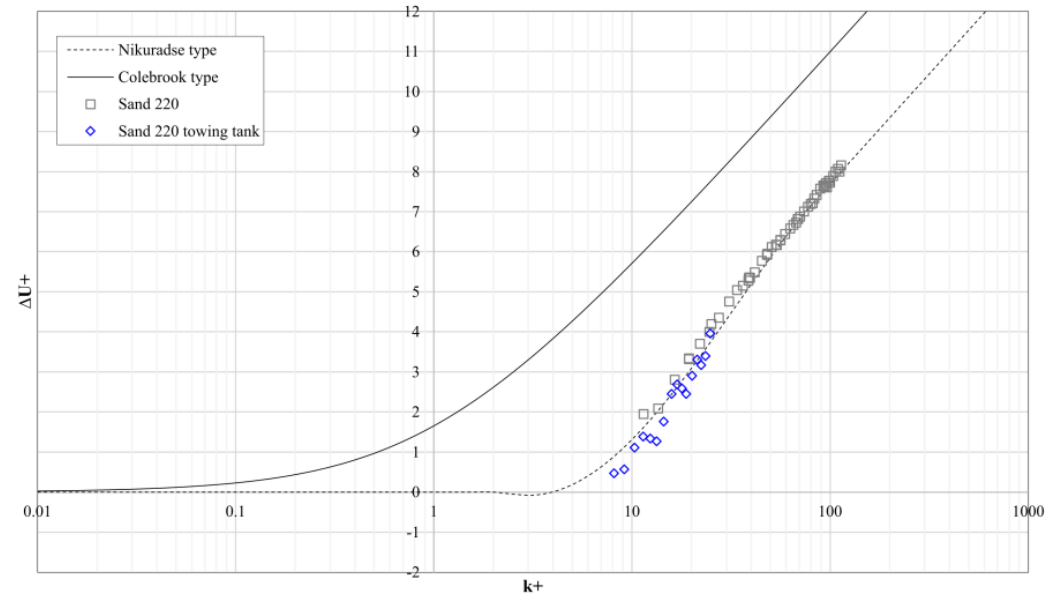


Figure 9. Experimental roughness function of the *Sand 220* surface developed from FTFC pressure drop measurements and from towing tank tests in [24].

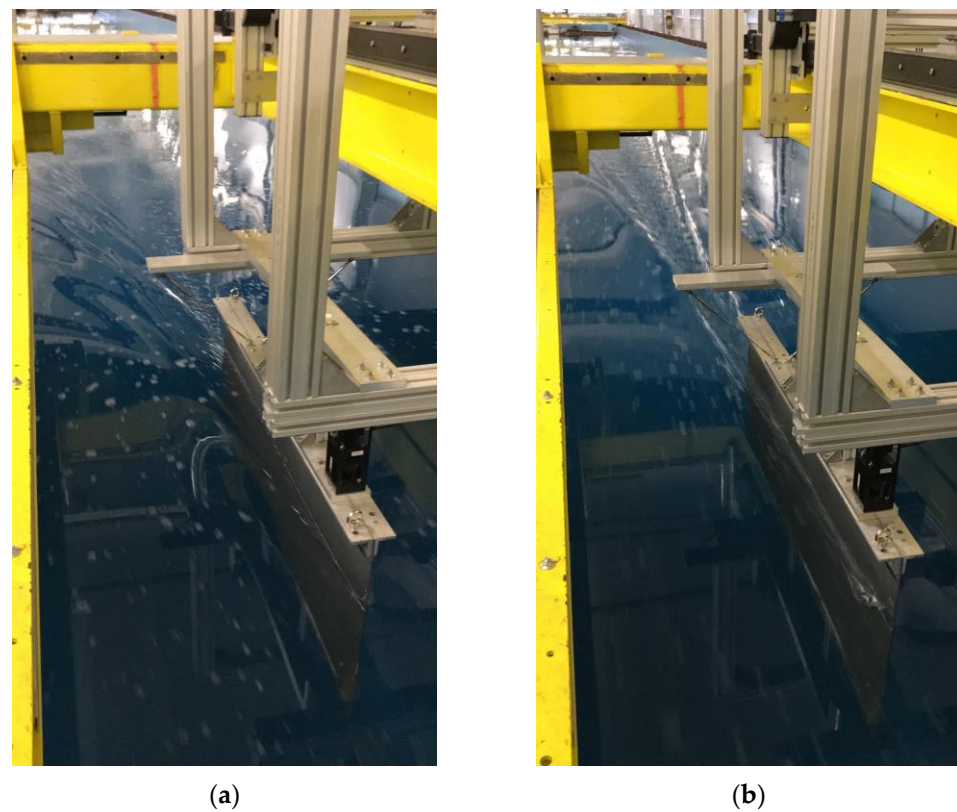
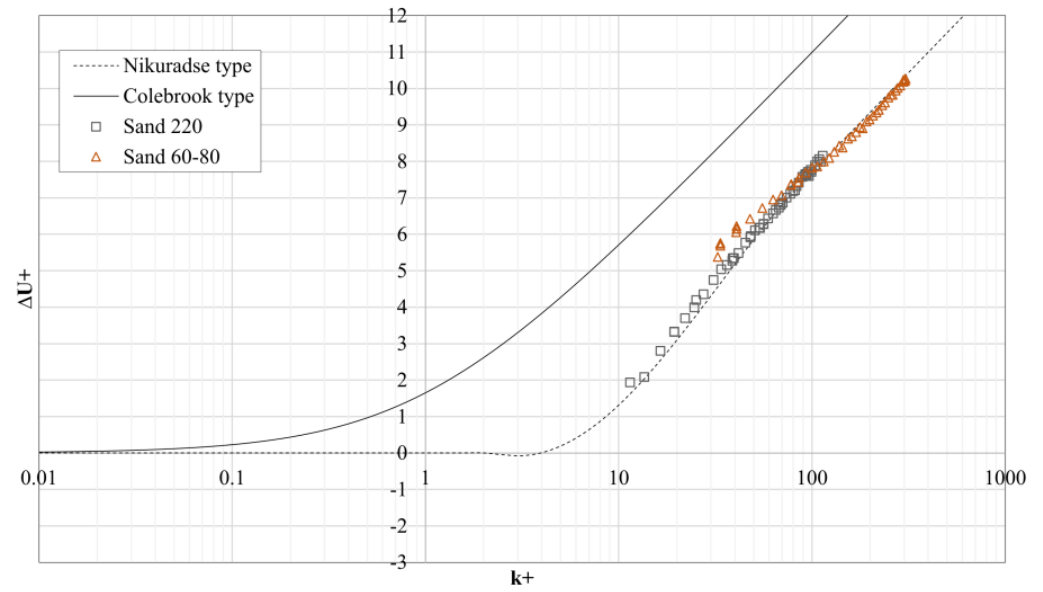


Figure 10. Towing tank experiments of a flat plate coated with *Sand 220* towed at: (a) 1.5 m/s; (b) 4.5 m/s used for comparison with the present FTFC tests [24].

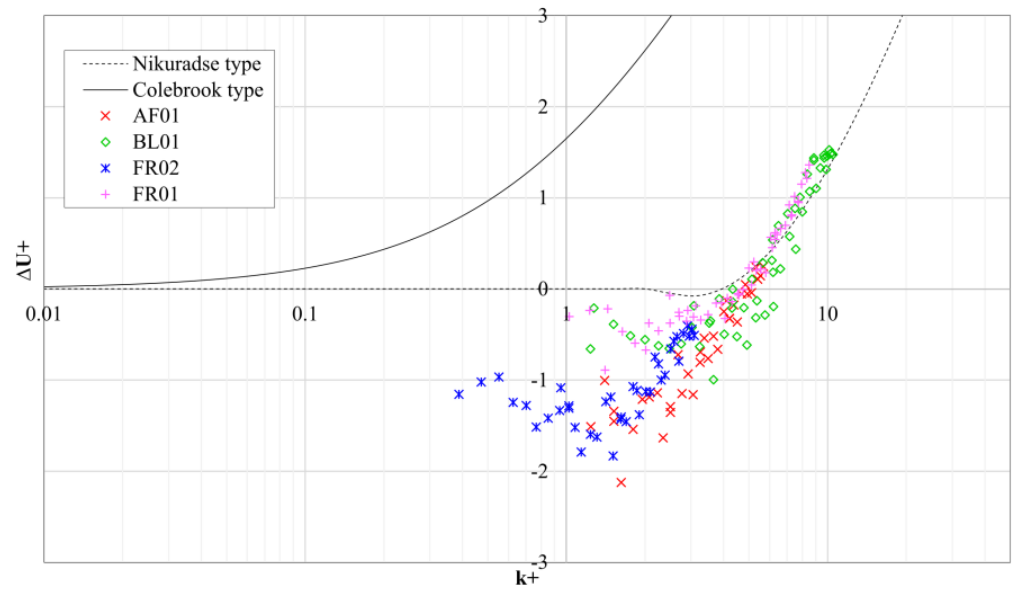
Similar to Figure 9, Figure 11 shows the experimental roughness functions, ΔU^+ , vs. roughness Reynolds numbers, k^+ obtained from the FTFC pressure drop measurements following Granville’s approach [14]. Notably, the experimental roughness functions of the FCCs tested (Figure 11b) show a deviation between the experimental results with Nikuradse in the vicinity of 0.4 to 5 (k^+). This is probably due to the special amphiphilic and hydrophobic characteristics of the coatings, which exhibited lower friction than the smooth reference. To overcome the deviation from Nikuradse’s model, the roughness functions were modelled by adapting the roughness function model of [43] with the curve fitting coefficients in Table 6. Finally, as previously mentioned, the roughness length scale values, k , were selected so that the roughness function models obtained were in agreement with the Nikuradse [15,33] or Colebrook type [35], Table 6. An exaggerated difference between the roughness functions of the smoothest and roughest coated panels is given in Figure 12.

Table 6. Curve fitting coefficients of the roughness functions for the test surfaces.

Test Surface	Roughness Length Scale, k [m]
<i>AF01</i>	$9.598 \cdot 10^{-6}$
<i>BL01</i>	$1.822 \cdot 10^{-5}$
<i>FR01</i>	$1.544 \cdot 10^{-5}$
<i>FR02</i>	$5.840 \cdot 10^{-6}$
<i>Sand 220</i>	$1.532 \cdot 10^{-4}$
<i>Sand 60-80</i>	$3.530 \cdot 10^{-4}$



(a)



(b)

Figure 11. Experimental roughness functions of the test surfaces developed from FTFC pressure drop measurements; (a) sanded rough; (b) FCCs.

3.2. Numerical Prediction on Full-Scale KCS Hull

3.2.1. Ship Resistance Coefficients

Numerical predictions were conducted on the benchmark KRISO containership hull at a towing speed of 24 knots (12.35 m/s), Froude number $Fn = 0.26$. The Reynolds number based on the ship speed and length was in the range of $Re_L = 2.72 \times 10^9$, which corresponds to the design speed of the full-scale KCS hull. Table 7 presents the particulars of the full-scale and model KCS adapted from Kim et al. [44].

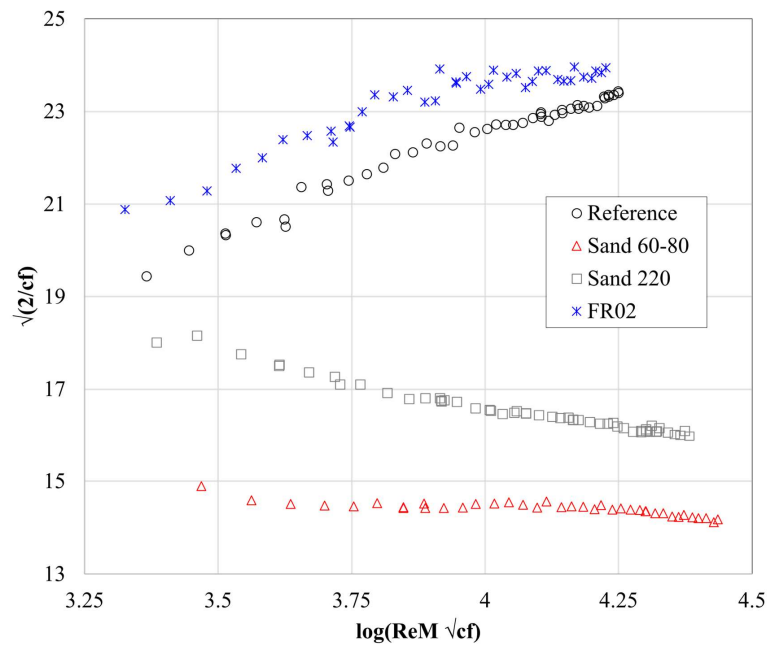


Figure 12. Exaggerated difference between the roughness functions of the smoothest and roughest coated panels.

The variance of resistance and powering requirements due to different test surfaces were calculated using Granville’s similarity law. It is of note that the newly developed roughness functions were incorporated into the procedure. Finally, the following Equations (11)–(18) were used to calculate the ship resistance coefficients similar to [45]. The total ship resistance coefficient, C_T , is defined in Equation (11) as a function of the total drag, R_T , the dynamic pressure, $1/2 \rho V^2$, and the hull wetted surface area, S :

$$C_T = \frac{R_T}{1/2 \rho S V^2} \tag{11}$$

where, V is the towing speed (i.e., the inlet velocity). It is well-known that the total ship resistance coefficient, C_T , can be decomposed into the frictional, C_F , and the residuary, C_R resistance coefficients, as given by Equation (12):

$$C_T = C_F + C_R \tag{12}$$

In the present study, the C_F values in Granville’s approach are calculated iteratively solving the Schoenherr smooth friction line, Equation (13):

$$0.242 C_F = \text{Log}(Re \cdot C_F) \tag{13}$$

where, Re is the Reynolds number based on ship speed and ship length at the waterline.

Consequently, the residuary resistance coefficients, C_R are calculated as in Equation (14):

$$C_R = C_T - C_F \tag{14}$$

The variation of the frictional resistance coefficient ΔC_F is the difference between the rough, $C_{F_{rough}}$, and smooth, $C_{F_{smooth}}$, conditions at the same Froude number can be given by Equation (15):

$$\Delta C_F = C_{F_{rough}} - C_{F_{smooth}} \tag{15}$$

Hence, the variation of the frictional resistance due to the presence of roughness can also be expressed in percentage, as in Equation (16)

$$\% \Delta C_F = \frac{C_{F_{rough}} - C_{F_{smooth}}}{C_{F_{smooth}}} \cdot 100 \tag{16}$$

The total resistance for the rough ship, $C_{T_{rough}}$, is determined by:

$$C_{T_{rough}} = C_{T_{smooth}} + \Delta C_T \tag{17}$$

where the total roughness allowance, ΔC_T is the variation in the total resistance coefficient between the rough, $C_{T_{rough}}$, and smooth, $C_{T_{smooth}}$, conditions, and can be given by Equation (18):

$$\Delta C_T = C_{T_{rough}} - C_{T_{smooth}} \tag{18}$$

Table 7. KRISO Container Ship (KCS) full-scale principal characteristics.

Parameters		
Scale factor	λ	1
Length between the perpendiculars	L_{PP} (m)	230
Length of waterline	L_{WL} (m)	232.5
Beam at waterline	B_{WL} (m)	32.2
Depth	D (m)	19.0
Design draft	T (m)	10.8
Wetted surface area w/o rudder	WSA_{Total} (m ²)	9424
Displacement	∇ (m ³)	52,030
Block coefficient	C_B	0.6505
Design speed	V (kn; m/s)	24; 12.35
Froude number	F_n	0.26
Reynolds number	Re	$2.72 \cdot 10^9$
Centre of gravity	KG (m)	7.28
Metacentric height	GM (m)	0.6

Figures 13 and 14, shows the resistance coefficients of the test cases obtained from the Granville’s similarity law compared to a hydrodynamically smooth ship hull. Interestingly, the test cases *AF01* and *FR02* show a negative ΔC_T of 2.3% and 3.8%, respectively. As expected, the phenomena of reduced ΔC_T values are due to the negative roughness functions, ΔU^+ observed from the experimental measurements. On the other hand, the *BL01* and *FR01* cases lead to light ΔC_T increases (0.7% for *BL01* and 0.2% for *FR01*) compared to the total added resistance due to mimicked slime (27.0% for *Sand 220* and 38.9% *Sand 60-80* cases). It can be noted that the *FR02* is the best performing FCCs tested while the sanded surface, *Sand 60-80*, leads to a higher increase in the total resistance coefficients.

It is notable that the total resistance coefficient results are in good agreement and show similar trends to the frictional resistance coefficients. Tables 8 and 9 present the frictional and total resistance coefficients obtained for the test surfaces. Furthermore, the results are reasonably in agreement with other studies found in the literature such as [16,22] found that a foul-release coating as applied measured an added frictional resistance $\% \Delta C_F$ equal to 2.6%, and for a 150 m flat plate at 12 knots coated with *Sand 60-80* calculated $\% \Delta C_F = 59\%$.

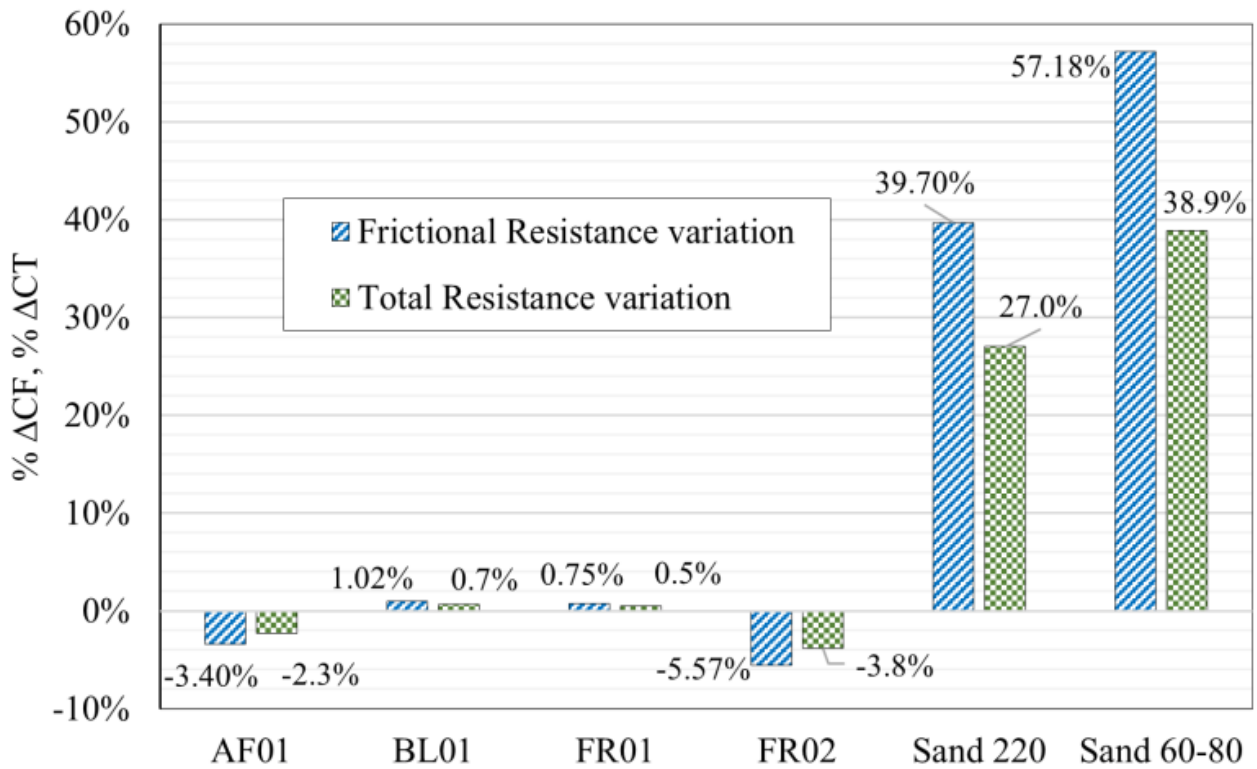


Figure 13. Frictional and total resistance coefficients variation in different hull roughness conditions.

Table 8. Frictional resistance results (C_F) results on the full-scale KCS hull at 24 knots ($Fn = 0.26$).

Test Surface	C_F	Granville Similarity Law	
		ΔC_F	$\% \Delta C_F$
Reference	$1.358 \cdot 10^{-3}$	-	-
AF01	$1.312 \cdot 10^{-3}$	$-4.620 \cdot 10^{-5}$	-3.40%
BL01	$1.378 \cdot 10^{-3}$	$1.387 \cdot 10^{-5}$	1.02%
FR01	$1.368 \cdot 10^{-3}$	$1.013 \cdot 10^{-5}$	0.75%
FR02	$1.282 \cdot 10^{-3}$	$-7.557 \cdot 10^{-5}$	-5.57%
Sand 220	$1.897 \cdot 10^{-3}$	$5.390 \cdot 10^{-4}$	39.70%
Sand 60-80	$2.135 \cdot 10^{-3}$	$7.765 \cdot 10^{-4}$	57.18%

Table 9. Total resistance coefficients of the full-scale KCS at 24 knots ($Fn = 0.26$).

Test Surface	C_T	Granville Similarity Law	
		ΔC_T	$\% \Delta C_T$
Reference	$1.996 \cdot 10^{-3}$	-	-
AF01	$1.950 \cdot 10^{-3}$	$-4.096 \cdot 10^{-5}$	-2.31%
BL01	$2.010 \cdot 10^{-3}$	$1.860 \cdot 10^{-5}$	0.69%
FR01	$2.006 \cdot 10^{-3}$	$4.668 \cdot 10^{-6}$	0.51%
FR02	$1.920 \cdot 10^{-3}$	$-7.096 \cdot 10^{-5}$	-3.79%
Sand 220	$2.535 \cdot 10^{-3}$	$5.320 \cdot 10^{-4}$	27.01%
Sand 60-80	$2.772 \cdot 10^{-3}$	$7.210 \cdot 10^{-4}$	38.90%

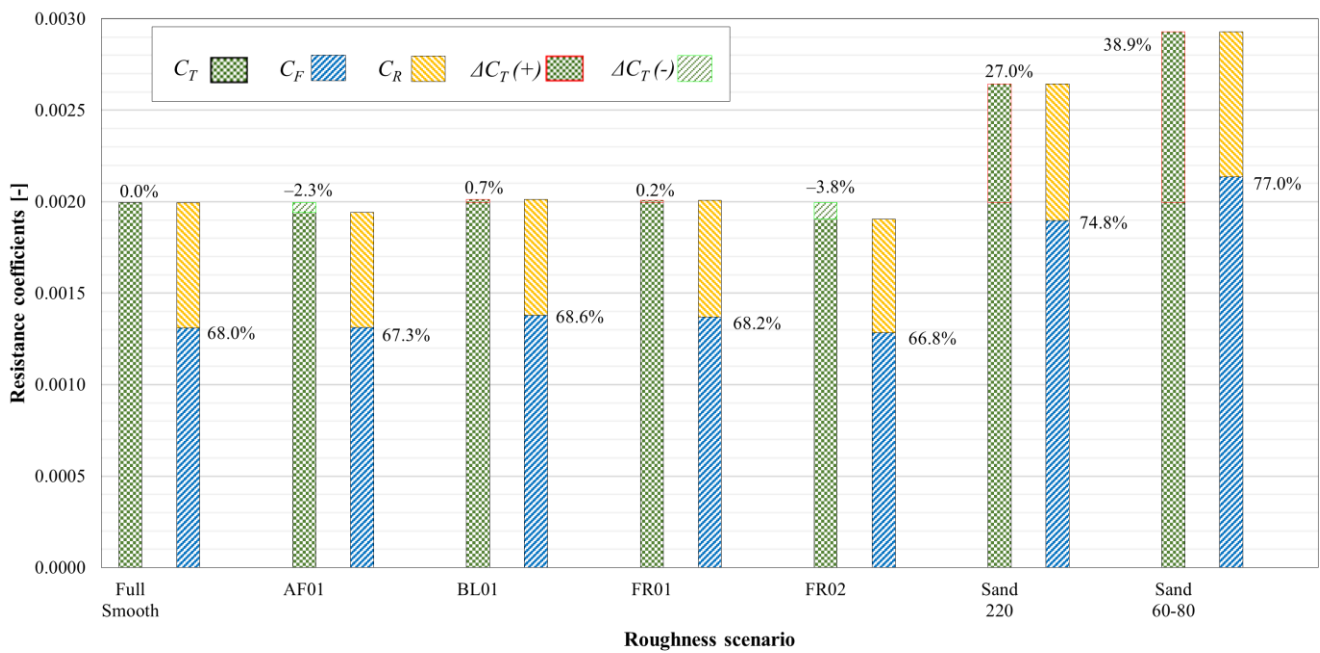


Figure 14. Percentage bar diagram of the resistance coefficients in different hull roughness conditions.

3.2.2. Ship Effective Power, ΔP_E

The change in effective power, $\% \Delta P_E$ due to the different surfaces tested can be expressed by:

$$\% \Delta P_E = \frac{C_{T_{rough}} - C_{T_{smooth}}}{C_{T_{smooth}}} \cdot 100 = \frac{\Delta C_T}{C_{T_{smooth}}} \cdot 100 \quad (19)$$

similar to that used by [46], where $C_{T_{smooth}}$ is the total resistance coefficient of the hull in smooth conditions obtained from CFD simulations. It is of note that $\% \Delta P_E$ is equal to $\% \Delta C_T$. Table 10 show the change in effective power, $\% \Delta P_E$ due to the different test cases obtained from Granville’s approach. It is of note that the largest difference between coating types for powering requirements is an average of 4.48%, between *FR02* and *BL01*. If the coatings *AF01* and *FR02* were applied on the ship hull, they would lead to a reduction in effective power requirements. In fact, *AF01* guarantees a maximum decrease of power requirements of 2.31%, while *FR02* of 3.79%.

Table 10. Effective power variation ($\% \Delta P_E$) of the full-scale KCS at 24 knots ($Fn = 0.26$).

Test Surfaces	$\% \Delta P_{E_{Granville}}$
<i>AF01</i>	−2.31%
<i>BL01</i>	0.69%
<i>FR01</i>	0.51%
<i>FR02</i>	−3.79%
<i>Sand 220</i>	27.01%
<i>Sand 60-80</i>	38.90%

As expected, the phenomena are due to the negative roughness functions, ΔU^+ observed from the experimental measurements to which correspond negative ΔC_T values. On the other hand, the *BL01* and *FR01* cases lead to positive $\% \Delta P_E$, which translates into increases in effective power requirements of 0.69% and 0.51%, respectively. Furthermore, the total added effective power due to mimicked slime is 27.01% for *Sand 220* and 38.90% *Sand 60-80* cases. The *FR02* is the best performing FCCs assessed ($\% \Delta P_E = -3.79\%$), while the sanded surface, *Sand 60-80*, would lead to the highest increase in the effective power

($\% \Delta P_E = 38.90\%$). Finally, it can also be noted that the rate $\% \Delta P_E / \% \Delta C_F$ is in the range of $65\% \div 70\%$, as would be expected [27].

4. Conclusions

An experimental and numerical study was conducted to investigate the full ship hydrodynamic performance of different fouling control coatings and mimicked biofouling. The investigation presented had five key tasks: physically conducting the pressure drop measurements experiment, calculating the skin friction coefficient, calculating the roughness functions, and implementing numerical methods.

The present study confirmed that the most rational approach to tackling the effect of ship hull roughness, including biofouling, is to combine experimental and numerical methods. The practical and sophisticated FTFC facility recently installed at the UoS was adopted for this scope. In fact, novel roughness functions for a novel hard foul-release coating, other commonly used marine coatings, and mimicked biofouled hull conditions were developed. Furthermore, this paper exploited the advantages of FTFC experiments to predict the effect hull roughness on full-scale ship resistance and powering. To the best of author's knowledge, only limited (and unpublished) research were conducted using the FTFC of the UoS before the present study. Hence, the urgency of using the FTFC designed and custom-built [19] at the University of Strathclyde (UoS). Furthermore, the experimental data produced supports drag reduction studies, and contributes to the international database of the roughness functions for different FCCs and biofouling. Producing experimental data was indeed recommended, e.g., by the 21st ITTC Surface Treatment Committee [20]. Finally, the goal of developing transferrable expertise with the FTFC of the UoS was met.

Hence, the experimental part of the study led to the introduction of novel experimental roughness functions for the FCCs tested including GIT's (*FR02* novel hard foul-release coating). Each surface's wall shear stress values and specific friction coefficients relative to the smooth uncoated reference surface were presented for completeness. Furthermore, the roughness function developed for a sandpaper-like surface (*Sand 220*) from the FTFC experiments was compared with previous towing tank tests. It is of note that this was the first time the same surface was tested in two different facilities of KHL. Therefore, the present study also confirmed the robustness of the FTFC (instead of a towing tank) combined with Granville's method to predict the effect of hull roughness on ship resistance and powering.

On the other hand, the numerical part of the study scaled up the laboratory results to the size of a full ship length. It is of note that the numerical predictions were conducted adopting Granville's similarity law scaling procedure based on the experimental results. In fact, the frictional resistance results for the FTFC experiments were used to determine the novel roughness functions for each test surface. The benchmark KRISO containership (KCS) hull in full-scale was chosen to calculate the variance of resistance and powering requirements due to different test surfaces at the design speed of 24 knots ($Fn = 0.26$).

Among the four fouling control coatings (FCCs) that were tested in the FTFC, the *FR02* coating (hard foul-release) displayed the best hydrodynamic performance across the entire Reynolds number range. In fact, the *FR02* coating displayed lower frictional resistance coefficients than if the ship was considered as smooth as the acrylic reference panel (5.57% decrease). Furthermore, the *FR02* surface led to a maximum decrease in effective power requirements of 3.79%. The results of the numerical prediction also show that the *AF01* (self-polishing antifouling coating) have better hydrodynamic performance than the smooth reference case (maximum decrease in effective power requirements of 2.31%). In contrast, *Sand 220* (medium light slime) and *Sand 60-80* (medium slime) have, as expected, the highest resistance due to their rougher characteristics. In fact, a ship hull with medium light slime (*Sand 220*) and medium slime (*Sand 60-80*) surface roughness characteristics as the test surfaces would experience a maximum increase in effective power requirements of 27.01% and 38.90%, respectively. Finally, it is of note that the Granville

method is limited to the assumption that the velocity is constant for the length of the plate (i.e., ship).

Further investigation could also be conducted on the prediction of resistance of the fouling control coatings (FCCs) at different speeds, on different hulls, and using heterogeneous patch distribution of the roughness [47]. It would also be beneficial to investigate the hydrodynamic performance of the same FCC under the effect of biofouling growth. Exposing surfaces to dynamically grown biofouling would give shipowners and operators a better indication of what powering penalty they should expect from these coatings after a certain time in active service. It is of note that such real biofouling could soon be simulated in the biofouling farm under development at the University of Strathclyde. Applying different mimicked biofouling to the panels before or after the coating application could also serve as a better method to predict the resistance behaviour of the as-applied condition to an existing rough ship hull.

Above all, the present study has provided several important findings, including the procedure to conduct pressure drop measurements with an FTFC, the application of Granville's method for pipes to develop roughness functions, as well as the introduction of roughness functions for a novel or widely adopted marine surfaces and mimicked biofouling. The findings presented can help predict the required power, fuel consumption and greenhouse gas emissions of ships with hulls coated with certain fouling control coatings and/or in the fouled condition. As a final remark, the authors would like to emphasise that there is an enormous opportunity for growth in the area of research on FTFCs. Indeed, the present study only represents an infinitesimal fraction of the number of coating products and surface roughness conditions that can be tested.

Author Contributions: Conceptualization, R.R., R.I. and S.S.; methodology, R.R., R.I. and S.S.; software, R.R.; validation, R.R. and R.I.; formal analysis, R.R. and R.I.; investigation, R.R. and S.S.; resources, C.J. and Y.K.D.; data curation, R.R. and R.I.; writing—original draft preparation, R.R.; writing—review and editing, R.R., R.I., M.A., Y.K.D. and T.T.; visualization, R.R.; supervision, C.J. and Y.K.D.; project administration, C.J. and Y.K.D.; funding acquisition, C.J., Y.K.D., S.S., M.A. and T.T. All authors have read and agreed to the published version of the manuscript.

Funding: This research was funded by EU H2020 project, VENTuRE (grant no. 856887, <https://h2020venture.eu/>, accessed on 25 November 2022), and it also supported by Inha University Research Grant (<http://eng.inha.ac.kr/>, accessed on 25 November 2022). This research was supported by the 'Development of Autonomous Ship Technology (20200615)' funded by the Ministry of Oceans and Fisheries (MOF, Republic of Korea).

Institutional Review Board Statement: Not applicable.

Informed Consent Statement: Not applicable.

Data Availability Statement: The authors confirm that the data supporting the findings of this study are available within the article.

Acknowledgments: The research presented in this paper was carried out as a collaboration across the University of Strathclyde (<https://www.strath.ac.uk/>, accessed on 25 November 2022) and Dalhousie University (<https://www.dal.ca/>, accessed on 25 November 2022), with the support of Graphite Innovation and Technologies (<https://www.graphiteenterprise.ca/>, accessed on 25 November 2022). Furthermore, the authors gratefully acknowledge: Chang Li (chang.li@ncl.ac.uk), Serkan Turkmen (serkan.turkmen@ncl.ac.uk) and the staff of the Hydrodynamics Laboratory of the University of Newcastle, for hosting the roughness measurement campaign; Claire De Marco Muscat-Fenech (claire.demarco@um.edu.mt), University of Malta, for securing additional funding to publish this research. Also, the results were obtained using the ARCHIE-WeSt High-Performance Computer (www.archie-west.ac.uk, accessed on 25 November 2022).

Conflicts of Interest: The authors declare no conflict of interest.

Nomenclature

C_T	Total resistance coefficient (ship)
C_F	Frictional resistance coefficient (ship)
C_R	Residuary resistance coefficient (ship)
P_E	Effective power (ship)
Re_L	Reynolds number (ship)
R_a	Mean roughness amplitude
k	Roughness length scale
k^+	Roughness Reynolds number
ΔU^+	Roughness function
Re_M	Reynolds number (panel)
c_f	Skin friction coefficient (panel)
R^2	Coefficient of determination
τ_w	Wall shear stress
U_τ	Friction velocity based on wall shear stress
D_h	Hydraulic diameter
Δp	Pressure drops value
Δx	Streamwise pressure gauges distance
U_M	Mean bulk velocity of the flow in the test section
h	Channel height
b	Channel beam
κ	von-Karman constant
ν	Kinematic viscosity
ρ	Density
U_A	Total uncertainty
P_A	Precision uncertainty limit
B_A	Bias uncertainty limit
Superscript	
+	Inner variable (normalized with U_τ)
Subscript	
smooth (s)	Smooth surface
rough (r)	Rough surface
Acronym	
FTFC	Fully Turbulent Flow Channel
CFD	Computational Fluid Dynamics
FCC	Fouling Control Coating
KRISO	Korea Research Institute of Ships & Ocean engineering
KCS	KRISO Container Ship
KVLCC2	KRISO Very Large Crude Carrier 2
UoS	University of Strathclyde
NAOME	Naval Architecture, Ocean and Marine Engineering
KHL	Kelvin Hydrodynamics Laboratory
DU	Dalhousie University
GIT	Graphite Innovation and Technology
AF01	Anti-Fouling 01 (Self-Polishing antifouling coating)
BL01	Boundary-Layer 01 (Gelcoat barrier coating)
FR01	Foul-Release 01 (Soft foul-release coating)
FR02	Foul-Release 02 (Hard foul-release coating)
Sand 220	Aluminium oxide sand grit 220 (Medium light slime surface)
Sand 60-80	Aluminium oxide sand grit 60-80 (Medium slime surface)

Appendix A

Figure A1 provides surface topography maps for the surfaces tested. The maps are of 90 mm by 40 mm. The vertical colour scale for surface elevation represents the unfiltered surface roughness.

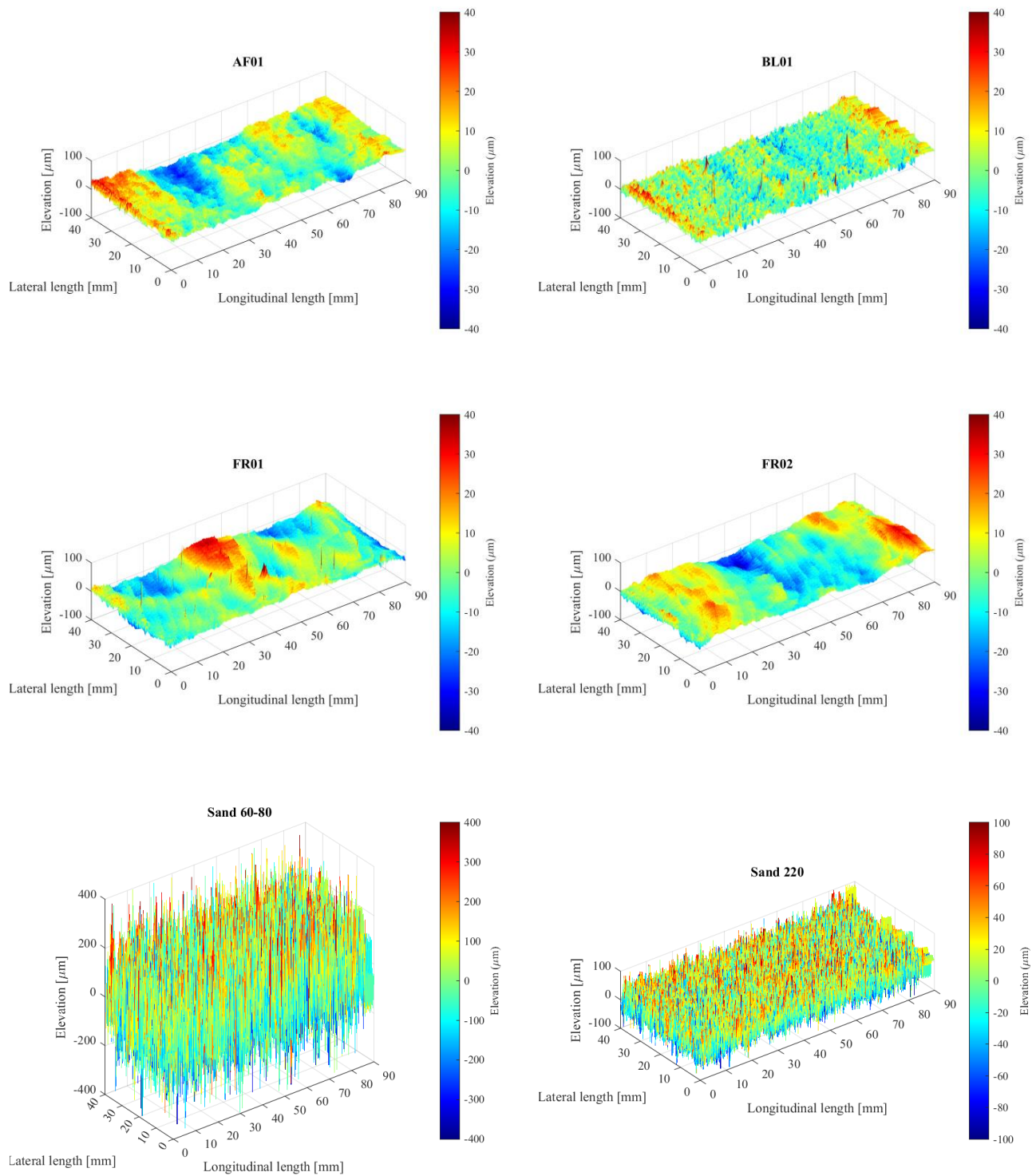


Figure A1. Unfiltered surface topography maps of the test surfaces.

References

- Schultz, M.P. Effects of Coating Roughness and Biofouling on Ship Resistance and Powering. *Biofouling* **2007**, *23*, 331–341. [CrossRef]
- IMO Resolution MEPC.328(76)—Revised MARPOL Annex VI. 2021. Available online: <https://www.ccs.org.cn/ccswzen/specialDetail?id=202206220255211398> (accessed on 30 October 2022).
- Song, S. *Development of Computational and Experimental Techniques to Investigate the Effect of Biofouling on Ship Hydrodynamic Performance*; University of Strathclyde: Glasgow, UK, 2020.
- Granville, P.S. *Similarity-Law Characterization Methods for Arbitrary Hydrodynamic Roughnesses*; Bethesda: Rockville, MD, USA, 1978.
- Granville, P.S. The Frictional Resistance and Turbulent Boundary Layer of Rough Surfaces. *J. Sh. Res.* **1958**, *2*, 52–74. [CrossRef]

6. Demirel, Y.K. *Modelling the Roughness Effects of Marine Coatings and Biofouling on Ship Frictional Resistance*; University of Strathclyde: Glasgow, UK, 2015.
7. Oliveira, D.; Larsson, A.I.; Granhag, L. Effect of Ship Hull Form on the Resistance Penalty from Biofouling. *Biofouling* **2018**, *34*, 262–272. [[CrossRef](#)]
8. Song, S.; Dai, S.; Demirel, Y.K.; Atlar, M.; Day, S.; Turan, O. Experimental and Theoretical Study of the Effect of Hull Roughness on Ship Resistance. *J. Sh. Res.* **2021**, *65*, 62–71. [[CrossRef](#)]
9. Lindholdt, A.; Dam-Johansen, K.; Olsen, S.M.; Yebra, D.M.; Kiil, S. Effects of Biofouling Development on Drag Forces of Hull Coatings for Ocean-Going Ships: A Review. *J. Coatings Technol. Res.* **2015**, *12*, 415–444. [[CrossRef](#)]
10. Yeginbayeva, I.A.; Granhag, L.; Chernoray, V. Review and Historical Overview of Experimental Facilities Used in Hull Coating Hydrodynamic Tests. *J. Eng. Marit. Environ.* **2018**, *233*, 1240–1259. [[CrossRef](#)]
11. Dean, R.B. Reynolds Number Dependence of Skin Friction and Other Bulk Flow Variables in Two-Dimensional Rectangular Duct Flow. *J. Fluids Eng.* **1978**, *100*, 215–223. [[CrossRef](#)]
12. Zanon, E.S.; Nagib, H.; Durst, F. Refined Cf Relation for Turbulent Channels and Consequences for High-Re Experiments. *Fluid Dyn. Res.* **2009**, *41*, 021405. [[CrossRef](#)]
13. Flack, K.A.; Schultz, M.P.; Barros, J.M.; Kim, Y.C. Skin-Friction Behavior in the Transitionally-Rough Regime. *Int. J. Heat Fluid Flow* **2016**, *61*, 21–30. [[CrossRef](#)]
14. Granville, P.S. Three Indirect Methods for the Drag Characterization of Arbitrarily Rough Surfaces on a Flat Plates. *J. Sh. Res.* **1987**, *31*, 70–77. [[CrossRef](#)]
15. Cebeci, T.; Bradshaw, P. *Momentum Transfer in Boundary Layers*; Hemisphere Publishing Corp.: Washington, DC, USA; McGraw-Hill Book Co.: New York, NY, USA, 1977; 407p.
16. Yeginbayeva, I.A.; Atlar, M. An Experimental Investigation into the Surface and Hydrodynamic Characteristics of Marine Coatings with Mimicked Hull Roughness Ranges. *Biofouling* **2018**, *34*, 1001–1019. [[CrossRef](#)]
17. Yeginbayeva, I.; Brink, A.; Emilie, V. New Measurement Facility: Enhanced Skin-Friction Measurement over Large-Scale Plates in a Channel Flow. In Proceedings of the 6th Hull Performance & Insight Conference, Pontignano, Italy, 30 August–1 September 2021; pp. 149–160.
18. Zhang, Y.; Yeginbayeva, I.; Brink, A. Modelling and Simulation of the Effect of Antifouling Coating on Ship Resistance. In Proceedings of the 6th Hull Performance & Insight Conference HullPIC'21, Pontignano, Italy, 30 August–1 September 2021; pp. 41–47.
19. Marino, A.; Shi, W.; Atlar, M.; Demirel, Y.K. Design Specification, Commission and Calibration of the University of Strathclyde's Fully Turbulent Flow Channel (FTFC) Facility. In Proceedings of the 6th International Conference on Advanced Model Measurements Technologies for The Maritime Industry (AMT'19), Rome, Italy, 9–11 October 2019.
20. ITTC Specialist Committee on Surface Treatment—Final Report and Recommendations to the 26th ITTC. In Proceedings of the 26th ITTC—Volume II, Hamburg, Germany, 18–19 January 2011.
21. GIT Graphite Innovation and Technologies—Smart Protective Marine Coatings. Available online: <https://www.grapheneenterprise.ca/> (accessed on 25 November 2022).
22. Schultz, M.P. Frictional Resistance of Antifouling Coating Systems. *J. Fluids Eng. Trans. ASME* **2004**, *126*, 1039–1047. [[CrossRef](#)]
23. KCS Geometry and Conditions. Available online: http://www.simman2008.dk/KCS/kcs_geometry.htm (accessed on 25 November 2022).
24. Ravenna, R. *Experimental Investigation on the Effect of Biomimetic Tubercles and Roughness on the Hydrodynamics of a Flat Plate*; University of Strathclyde: Glasgow, UK; Università degli studi di Trieste: Trieste, Italy, 2019.
25. Song, S.; Demirel, Y.K.; De Marco Muscat-Fenech, C.; Tezdogan, T.; Atlar, M. Fouling Effect on the Resistance of Different Ship Types. *Ocean Eng.* **2020**, *216*, 107736. [[CrossRef](#)]
26. Yeginbayeva, I.A.; Atlar, M.; Turkmen, S.; Chen, H. Effects of 'in-Service' Conditions—Mimicked Hull Roughness Ranges and Biofilms—on the Surface and the Hydrodynamic Characteristics of Foul-Release Type Coatings. *Biofouling* **2020**, *36*, 1074–1089. [[CrossRef](#)]
27. Schultz, M.P.; Bendick, J.A.; Holm, E.R.; Hertel, W.M. Economic Impact of Biofouling on a Naval Surface Ship. *Biofouling* **2011**, *27*, 87–98. [[CrossRef](#)]
28. Schultz, M.P.; Walker, J.M.; Steppe, C.N.; Flack, K.A. Impact of Diatomaceous Biofilms on the Frictional Drag of Fouling-Release Coatings. *Biofouling* **2015**, *31*, 759–773. [[CrossRef](#)]
29. Howell, D.; Behrends, B. A Review of Surface Roughness in Antifouling Coatings Illustrating the Importance of Cutoff Length. *Biofouling* **2006**, *22*, 401–410. [[CrossRef](#)]
30. Li, C.; Atlar, M.; Haroutunian, M.; Anderson, C.; Turkmen, S. An Experimental Investigation into the Effect of Cu₂O Particle Size on Antifouling Roughness and Hydrodynamic Characteristics by Using a Turbulent Flow Channel. *Ocean Eng.* **2018**, *159*, 481–495. [[CrossRef](#)]
31. ITTC ITTC-Recommended Procedures—Fresh Water and Seawater Properties. In Proceedings of the 26th International Towing Tank Conference, Rio de Janeiro, Brazil, 28 August–3 September 2011; pp. 1–45.
32. Hama, F.R. *Boundary Layer Characteristics for Smooth and Rough Surfaces*; The Society of Naval Architects, SNAME, Paper No. 6 Paper; T1954-1 Transactions; Iowa Institute of Hydraulic, State University of Iowa: Iowa City, IA, USA, 1954.
33. Nikuradse, J. *Laws of Flow in Rough Pipes*; District of Columbia: Washington, DC, USA, 1933.

34. Schlichting, H.; Klaus, G. *Boundary Layer Theory*, 9th ed.; Springer: Braunschweig, Germany, 2017.
35. Colebrook, C.F.; Inst, A.M.C.E.; Thomas, M. A New Theory of Turbulent Flow in Liquids of Small Viscosity. *J. Inst. C.E* **1939**, *11*, 611.
36. ITTC Executive Committee. Final Report and Recommendations to the 27th ITTC. In Proceedings of the 27th ITTC Conference, Lima, Peru, 27 November–2 December 2014.
37. Coleman, H.W.; Steele, W.G. Engineering Application of Experimental Uncertainty Analysis. *AIAA J.* **2012**, *33*, 1888–1896. [[CrossRef](#)]
38. ITTC. ITTC Uncertainty Analysis, Example for Resistance Test. In *ITTC Recommended Procedures and Guidelines, Procedure 7.5-02-02-02, Revision 01*; ITTC: East, Kenya, 2002.
39. Schultz, M.P.; Flack, K.A. Reynolds-Number Scaling of Turbulent Channel Flow. *Phys. FLUIDS* **2013**, *25*, 25104. [[CrossRef](#)]
40. Walker, J.M.; Schultz, M.P.; Flack, K.A.; Steppe, C.N.; Academy, U.S.N. Skin-Friction Drag Measurements on Ship Hull Coating Systems. In Proceedings of the 30th Symposium on Naval Hydrodynamics, Hobart, Australia, 2–7 November 2014; pp. 2–7.
41. Grigson, C. Drag Losses of New Ships Caused by Hull Finish. *J. Sh. Res* **1992**, *36*, 182. [[CrossRef](#)]
42. Ravenna, R.; Marino, A.; Song, S.; Atlar, M.; Turan, O.; Day, S.; Demirel, Y.K. Experimental Study on the Effect of Biomimetic Tubercles on the Drag of a Flat Plate. *Ocean Eng.* **2022**, *255*, 111445. [[CrossRef](#)]
43. Demirel, Y.K.; Turan, O.; Incecik, A. Predicting the Effect of Biofouling on Ship Resistance Using CFD. *Appl. Ocean Res.* **2017**, *62*, 100–118. [[CrossRef](#)]
44. Kim, W.J.; Van, S.H.; Kim, D.H. Measurement of Flows around Modern Commercial Ship Models. *Exp. Fluids* **2001**, *31*, 567–578. [[CrossRef](#)]
45. Schultz, M.P.; Flack, K.A. The Rough-Wall Turbulent Boundary Layer from the Hydraulically Smooth to the Fully Rough Regime. *J. Fluid Mech.* **2007**, *580*, 381–405. [[CrossRef](#)]
46. Tezdogan, T.; Demirel, Y.K.; Kellett, P.; Khorasanchi, M.; Incecik, A.; Turan, O. Full-Scale Unsteady RANS CFD Simulations of Ship Behaviour and Performance in Head Seas Due to Slow Steaming. *Ocean Eng.* **2015**, *97*, 186–206. [[CrossRef](#)]
47. Ravenna, R.; Song, S.; Shi, W.; Sant, T.; De Marco Muscat-Fenech, C.; Tezdogan, T.; Demirel, Y.K. CFD Analysis of the Effect of Heterogeneous Hull Roughness on Ship Resistance. *Ocean Eng.* **2022**, *258*, 111733. [[CrossRef](#)]